

PAPER • OPEN ACCESS

Simultaneous surface and bulk sensitive XAS measurements of magnetic particle clusters

To cite this article: S Swaraj *et al* 2017 *J. Phys.: Conf. Ser.* **849** 012014

View the [article online](#) for updates and enhancements.

Related content

- [Investigation of structural and electronic properties in Ru perovskite oxides by XAFS measurements](#)
M Mizumaki, K Yoshii, Y Hinatsu *et al.*
- [Using combined XAS/DRIFTS to study CO/NO Oxidation over Pt/Al₂O₃ catalysts](#)
A M Gänzler, H Lichtenberg, A I Frenkel *et al.*
- [Visualization of magnetic dipolar interaction based on scanning transmission X-ray microscopy](#)
Hiroyuki Ohtori, Kaoru Iwano, Chiharu Mitsumata *et al.*

Simultaneous surface and bulk sensitive XAS measurements of magnetic particle clusters

S Swaraj^{1*}, P M Dietrich² and W E S Unger²

¹Synchrotron SOLEIL, L'Orme des Merisiers, Saint-Aubin - BP 48, F-91192 Gif-sur-Yvette cedex, FRANCE

²BAM Federal Institute of Materials Research and Testing, 12200 Berlin, Germany

*sufal.swaraj@synchrotron-soleil.fr

Abstract. Magnetic iron oxide nanoparticle clusters (mnp) coated with organic stabilizers were investigated using scanning transmission x-ray microscopy (STXM). Simultaneous surface and bulk sensitive Fe L₃ edge absorption spectra, obtained using a photomultiplier tube and a channeltron, were used to detect subtle changes in the oxidation state in the surface and bulk of Iron Oxide mnp. The effectiveness of this mode of STXM operation is demonstrated for these nanoparticle clusters.

1. Introduction

The application of magnetic nanoparticles of 5-20 nm diameter and their clusters are actively investigated as Magnetic Resonance (MR) imaging contrast agents due to their low toxicity, high saturation magnetization, high magnetic susceptibility, biodegradability, ease of synthesis and functionalization [1]. However, small particle size also means a decrease in the saturation magnetization [2] and formation of ferromagnetic agglomerates. Stabilizers in a controlled manner are used to overcome the magnetic attraction and to form superparamagnetic clusters.

While the shape, size, agglomeration, coatings and other synthesis parameters are well understood and controlled [3], the interplay and transformation between different iron oxide phases in these nanoparticles clusters is largely uncontrolled and not fully understood. The existence of Fe²⁺ cations in these Fe₃O₄ (magnetite) magnetic nanoparticle clusters (mnp's) can lead to oxidation and conversion to γ -Fe₂O₃ (maghemite) and finally to α -Fe₂O₃ (hematite) that has no magnetic properties [4]. The iron oxide phase inside the bulk and at the surface of these clusters can have a significant effect on the overall magnetic properties. However, the similar spectroscopic and crystallographic signature of different iron oxides has withheld researchers from correlating magnetic properties with synthesis techniques.

In this paper we present the bulk sensitive and surface sensitive x-ray absorption based characterization of iron oxide (Fe_xO_y) mnp's coated with dopamine stabilizer. This detection methodology and experimental configuration (Figure 1e) has already been successfully applied for organic materials [5]. Bulk sensitivity was achieved by detection of photons transmitted through the whole samples using a photomultiplier tube. Simultaneous detection of emitted photoelectrons from the sample's surface was achieved using a channeltron. Since the escape depth of Fe 2p photoelectrons at the Fe L-edge is about 4.5 nm for iron oxide [6] the information depth corresponds to the top



surface of the investigated region. We have focused our studies on the Fe L-edge as it is highly sensitive to oxidation state of iron.

2. Experimental

STXM and X-ray absorption spectroscopy (XAS) measurements were performed at the Pollux beamline at the Swiss Light Source (SLS), Villigen, Switzerland [7]. A 35 nm zone plate (ZP) is used to focus the x-rays through an order sorter aperture (OSA) on to the sample. The mnp_c's were dropcasted on a 100 nm thick silicone nitride window for measurements. A scintillator coupled with a photomultiplier tube (indicated "PMT") is used to detect the bulk sensitive signal in the form of transmitted photons. Surface sensitivity was made possible by detecting surface photoelectrons using a channeltron (indicated "CT") biased at 2.5 kV (model no. KBL10RS, Dr. Sjuts Optotechnik GmbH). The CT was mounted adjacent to the PMT and the sample was mounted facing the detectors. A wet-cell sample was also prepared for dopamine coated mnp_c's and was measured only using the PMT. This particular sample was prepared by sealing a drop of mnp_c solution in a sandwich of two silicone nitride windows with epoxy. The chamber was pumped down to 10⁻⁶ mbar. The normalization of the CT signal was done by dividing it with the measured photon flux on the PMT. Measurements used in the present work are not intended to be quantitative in nature hence the photon energy dependence of the detector efficiencies was ignored. The PMT signal was normalized using signal from a blank silicone nitride window. The XAS spectra were extracted through line scans after choosing a sample region representative of the whole sample. Plasma treatment was done in an Atto plasma cleaner (Diener electronics GmbH) for 30 min using a H₂/He gas mixture at 0.6 mbar of H₂ and 100% power. Samples were transferred to the STXM experiment station with minimum exposure to ambient air.

3. Results and discussion

3.1. STXM imaging

STXM images obtained at 711 eV from the PMT and the CT are shown in figure 1 for the uncoated, and dopamine coated mnp_c's. The thickness of these coatings was calculated in a separated study on core shell nanoparticles to be ca. 1nm [8]. In general large clusters of several hundred nms in size and about 150 nm in thickness was observed in all the cases. Since these samples were drop-cast and air-dried, the analysed clusters are not perfectly dispersed. Several spectra were obtained through a line scan to ensure the chemical homogeneity of the sample before choosing representative spectra.

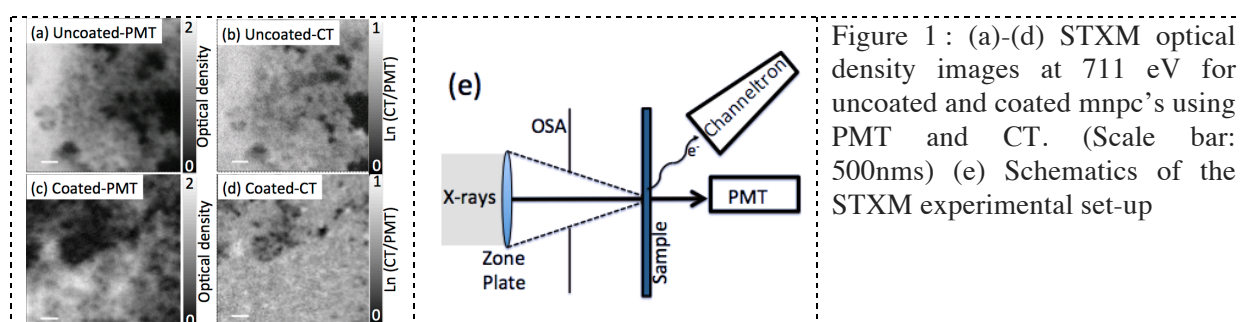


Figure 1: (a)-(d) STXM optical density images at 711 eV for uncoated and coated mnp_c's using PMT and CT. (Scale bar: 500nms) (e) Schematics of the STXM experimental set-up

3.2. Fe L₃ edge Absorption spectra

Figure 2a shows the Fe L₂₃ XAS spectra of uncoated and dopamine coated Fe_xO_y mnp_c's. Two regions corresponding to the L₃(2p_{3/2}) peak around 710 eV and L₂(2p_{1/2}) peak around 722 eV can be observed. The ligand field splitting and other atomic interactions form the basis of the fine structure within these regions [9]. We have focussed our discussion on the L₃ region of the spectra as there are significant differences in the PMT and CT signals in this region of the uncoated and dopamine coated mnp_c's. The A, B and C energy positions (Figure 2a,b) marked in the L₃ region correspond to site occupancies of Fe cations in the spinel structure. A corresponds to Fe²⁺ species at octahedral sites (Fe²⁺ O_h), B

corresponds to Fe^{3+} species at tetrahedral sites ($\text{Fe}^{3+} \text{T}_d$) and **C** corresponds to Fe^{3+} species at octahedral sites ($\text{Fe}^{3+} \text{O}_h$). Relative intensity differences can be observed around the feature **A**. The features **B** and **C** are not clearly resolved. In order to obtain a relative quantification of the oxidation state of iron in the mnp samples we have used the linear combination of simulated Fe^{2+} and Fe^{3+} spectra using the CTM4XAS software [10].

A linear combination of the simulated spectra of only two species, $\text{Fe}^{2+}(\text{O}_h)$ and $\text{Fe}^{3+}(\text{O}_h)$, were used to obtain a consistent fit. The simulation parameters were used according to ref. [9, 10]. A representative fitted spectrum is shown in figure 2b. The integrated intensity of each component is used to estimate the $\text{Fe}^{2+}/\text{Fe}^{3+}$ ratio. Figure 2c shows the $\text{Fe}^{2+}/\text{Fe}^{3+}$ ratios as obtained from the fits for all the spectra. These include the measurements on a reference maghemite sample (Fe_2O_3) and from a wet-cell sample wherein the dopamine-coated mnp's were dispersed in water. Firstly, it is evident that although the reference maghemite (Fe_2O_3) sample, measured in TEY (Total Electron Yield) mode, should be purely Fe^{3+} , it was necessary to introduce the Fe^{2+} component to obtain a reasonable fit. This could be due to reduced sites below the top surface of the reference sample. As expected, the Fe^{3+} phase is the dominant phase in the reference sample. Among the mnp's, the uncoated clusters show the maximum amount of Fe^{2+} species ($\text{Fe}^{2+}/\text{Fe}^{3+} \sim 0.9$). The bulk and the surface content of the two phases are not very different, with Fe^{3+} content slightly higher in the surface. This observation is expected since the surface is inevitably oxidised. Reduction by H_2 plasma results in an overall decrease in the Fe^{3+} content at the surface as well as in the bulk as illustrated by strong differences in the L_3 region. Figure 2b shows exemplarily the spectra of dopamine coated mnp's treated with H_2 plasma for 30 minutes.

In the case of dopamine coated mnp's, it is clear that the bulk content of Fe^{2+} is lower than the surface content of Fe^{2+} indicating a more oxidized bulk compared to the surface. Such behaviour is consistent with initial oxidation behaviour of magnetite as observed by McCarty et al. [11]. In general the transformation of iron oxide starting from magnetite (Fe_3O_4) to maghemite ($\gamma\text{-Fe}_2\text{O}_3$) can be described by the progressive oxidation of octahedral [Fe^{2+}] to [Fe^{3+}] by losing some structural iron and creating cation vacancies [12] according to the following substitutional series $[\text{Fe}^{3+}]_2\{\text{Fe}^{3+}_{1+2\delta}\text{Fe}^{2+}_{1-3\delta}\square_\delta\}\text{O}_4$ where $[\]$ indicates tetrahedral sites, $\{ \}$ indicates octahedral sites, \square represents cation vacancies in the spinel structure and $0 \leq \delta \leq 1/3$ [13]. This implies

$$\frac{Fe_{(Oh)}^{2+}}{Fe_{(Oh)}^{3+} + Fe_{(Td)}^{3+}} = \frac{1 - 3\delta}{2 + 2\delta} \quad (1)$$

δ values calculated for different samples are presented in figure 2c along with the theoretical values for pure magnetite and pure maghemite. Values of δ greater than $1/3$ and less than 0 indicate the presence of mixed phases not consistent with either magnetite or maghemite phases. The dopamine coated dry samples clearly show a magnetite like composition. The dopamine coated wet-cell sample shows the most maghemite like composition that is very different from dry dopamine mnp sample. This could be due to the fact that the wet cell sample was significantly older than the dry sample. This could have allowed for sufficient oxidation time for magnetite like mnp's. The uncoated sample's composition indicates the abundance of Fe^{2+} sites originating from neither magnetite nor maghemite phases but most probably from mixed iron oxide phases. It has to be noted that we have ignored the presence of metallic Fe^0 species in our fitting routine. The energy position of Fe^{2+} is closer to Fe^0 species and some of the contributions of Fe^{2+} species account also for the Fe^0 species, especially in the case of broad L_3 peaks obtained for uncoated mnps.

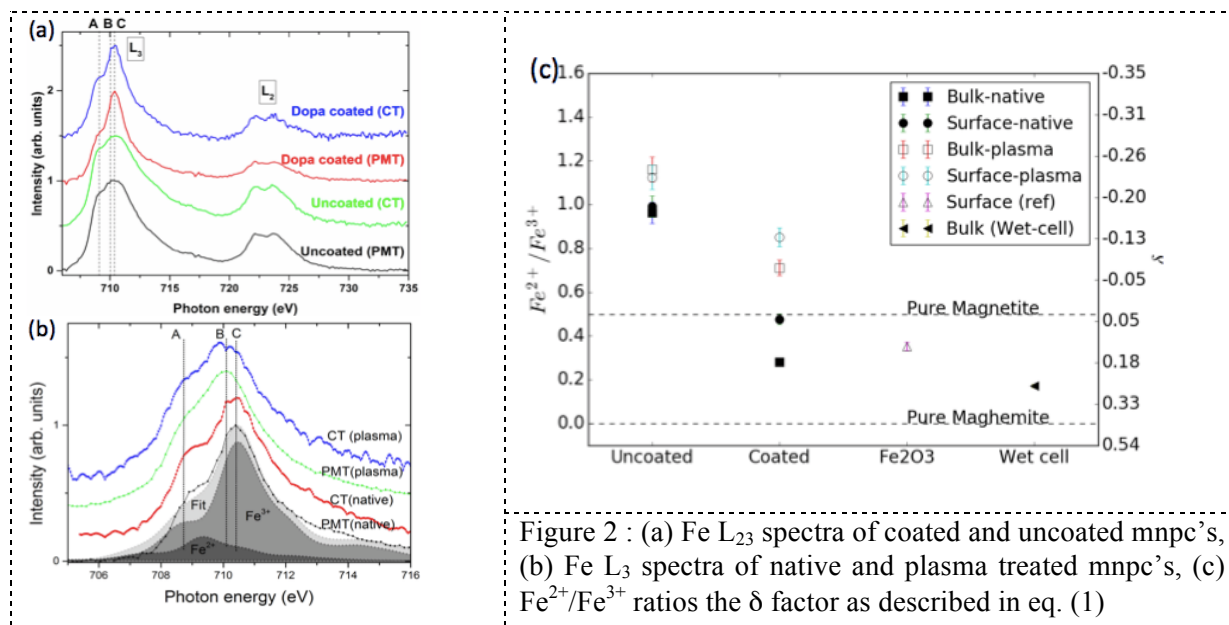


Figure 2 : (a) Fe L₂₃ spectra of coated and uncoated mnp's, (b) Fe L₃ spectra of native and plasma treated mnp's, (c) Fe²⁺/Fe³⁺ ratios the δ factor as described in eq. (1)

4. Conclusion

We have shown that using bulk and surface sensitive measurements in STXM, it is possible to disentangle subtle changes in oxidation state of iron oxide mnp's. Furthermore the applied characterization strategy of iron oxide based nanoparticles combined with computational simulations of Fe L₃ spectra allows distinguishing differently coated iron oxide np's in terms of iron oxide nature, especially of magnetite or maghemite characteristics. Dopamine coatings were found to introduce oxidation state changes leading to increase of Fe³⁺ species. Also mixed Fe_xO_y species were identified by simultaneous bulk and surface sensitive STXM/XAS measurements as demonstrated for the "naked" Fe_xO_y core particles.

References

- [1] Y. Sahoo et al., 2005, *J. Phys. Chem. B* **109** 3879; W. Ryoo et al. 2003, *Ind. Eng. Chem. Res.* **42** 6348; B.-S Kim et al. 2005, *Nano Lett.* **5** 1987; W. Zheng et al. 2005, *J. Magn. Magn. Mater.* **288** 403; G. Fritz et al. 2002, *Langmuir* **18** 6381; D. Reith et al. 2002, *J. Chem. Phys.* **116** 9100.
- [2] G. Vaidyanathan et al. 2007, *J. Magn. Magn. Mater.* **313** 293.
- [3] J. Park et al. 2005, *Angew. Chem.* **117** 2932; J. Park et al. 2004, *Nat. Mater.* **3** 891; B. H. Kim et al. 2011, *J. Am. Chem. Soc.* **133** 12624; L. M. Bronstein et al. 2011, *Langmuir* **27** 3044.
- [4] L. Signorini et al. 2003, *Phys. Rev. B* **68** 195423.
- [5] B. Watts et al. 2010, *Macromol. Rapid Commun.* **31** 1706.
- [6] S. Gota et al. 2000, *Phys. Rev. B* **62** 4187.
- [7] J. Raabe et al. 2008, *Rev. Sci. Instrum.* **79** 113704.
- [8] H. Kalbe et al. 2016, *J. Electron Spectrosc. Relat. Phenom.* **212** 34.
- [9] P. Kuiper et al. 1997, *J. Electron Spectrosc. Relat. Phenom.* **86** 107; R.A. Patrick et al. 2002, *Eur. J. Mineral.* **14** 1095; V.N. Antonov et al. 2003, *Phys. Rev. B* **67** 024417.
- [10] E. Stavitski et al. 2010, *Micron* **41** 687.
- [11] T. Fujii T et al. 1999 *Phys. Rev. B* **59** 3195.
- [12] K. F. McCarty et al. 2014 *J. Phys. Chem. C* 2014 **118** 19768.
- [13] G. P. Santana et al. 2001, *Cio Solo* **25** 33; N. Mahmed et al. 2014, *J. Magn. Magn. Mater* **353** 15.